

# INTRODUCTION OF A FLOW PENETRATION METRIC FOR EVALUATING THE IMPACT OF BUILDING COVERING VEGETATION ON WIND-DRIVEN NATURAL VENTILATION OF INDOOR SPACES

*C. Irrenfried<sup>1</sup>, V. Pappa<sup>2</sup>, C. Gromke<sup>3</sup> and D. Bouris<sup>2</sup>*

<sup>1</sup> *Institute of Fluid Mechanics and Heat Transfer, Graz University of Technology*

<sup>2</sup> *School of Mechanical Engineering, National Technical University of Athens*

<sup>3</sup> *Institute for Water and Environment, Karlsruhe Institute of Technology*

*c.irrenfried@tugraz.at*

## Abstract

The present study introduces the "penetration metric" as a novel approach for quantifying the ventilation efficiency of indoor spaces. This metric is employed to evaluate the influence of green façade vegetation on air exchange in an isolated building subjected to wind. Experiments were conducted in a wind tunnel, using a scaled cubic building model with opposing openings at the side walls. Various vegetation types with different permeabilities and thicknesses were applied to the windward façade. Airflow dynamics were analysed using Laser Doppler Velocimetry. The results demonstrate that façade vegetation substantially modifies the flow characteristics, particularly near the upstream building corner, where reductions in velocity fluctuations and turbulence intensity were observed. Moreover, it was found that denser vegetation more effectively dampens high-frequency turbulent structures. Comparison with measurements indicates that the penetration metric effectively accounts for these effects on the air exchange rate.

## 1 Introduction

Natural ventilation plays a crucial role in maintaining indoor air quality and thermal comfort in residential and commercial buildings. It relies on outdoor air movement to replace indoor air, thereby reducing pollutant concentrations and excess heat. This process significantly enhances energy efficiency by reducing dependence on mechanical ventilation systems.

Ventilation efficiency is typically investigated through on-site measurements, numerical simulations, or wind tunnel experiments, with the latter being particularly favoured due to the controlled conditions they offer. Ventilation efficiency – commonly quantified by the air change per hour (ACH) or airflow rate through an opening – can be directly determined using the concentration decay method (Larsen and Heiselberg, 2008; Bu et al., 2010; Pappa et al., 2023b; Stenech et al., 2025) or by measuring the local velocity field near the opening through optical techniques (Karava

et al., 2011; Manolesos et al., 2018; Albuquerque et al., 2020; Stenech et al., 2025).

Despite the increasing adoption of green roofs and façade greening as sustainable solutions for urban buildings, their impact on natural ventilation remains inadequately explored. Recent studies have begun to investigate the complex interactions between vegetation porosity, wind flow, and ventilation rates Li et al., 2022; Pappa et al., 2023b; Pappa et al., 2023a. Experimental results indicate that, regardless of species, vegetation on the façade and the roof influences the air exchange rate. Moreover, vegetation can modify airflow patterns around a building by altering surface roughness, turbulence characteristics, and pressure distributions near openings.

The present study introduces the "penetration metric" as a novel approach for quantifying the efficiency of ventilation of indoor spaces. Here, this metric is used to evaluate the impact of green façade vegetation on air exchange in an isolated building exposed to wind. Unlike conventional mean flow velocity metrics, which approach zero in fully fluctuating flow regimes, the penetration metric offers a more reliable measure of ventilation effectiveness.

## 2 Experimental approach

The experiments were conducted in an atmospheric boundary layer wind tunnel at the Laboratory of Building and Environmental Aerodynamics at the Institute for Water and Environment, Karlsruhe Institute of Technology, using a reduced-scale cubic model with an edge length of  $L = 110$  mm and openings on two opposite side walls, as shown in Figure 1.

The atmospheric boundary layer was simulated to represent an urban environment, with a reference velocity of  $U_{ref} = 3.27$  m/s measured upstream at the building height  $h = 110$  mm. Details about the boundary layer characteristics can be found in Pappa et al. (2023b). Various vegetation types applied to the upstream façade of the building are investigated in the present study. Vegetation is commonly charac-

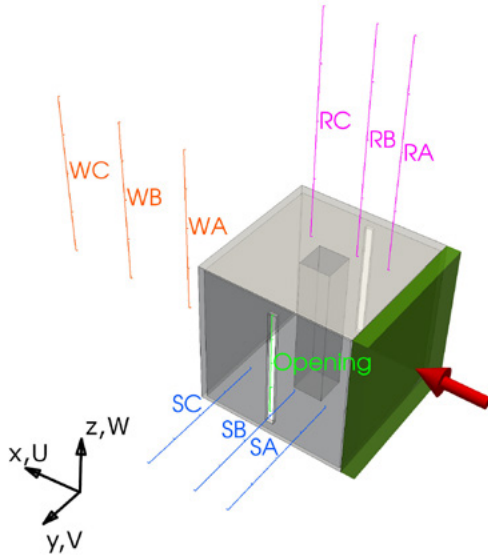


Figure 1: Model building and the LDV measurement positions

terised by its leaf area density (LAD,  $m^2/m^3$ ), as described in, e.g. Balczó et al. (2009). Real ivy façade greenery has been found to exhibit LAD values of up to  $10 m^2/m^3$ . In the present experiments, the vegetation was modelled using open-cell foam materials with varying permeabilities and thicknesses, as summarised in Table 1. Foams with pore per inch (PPI) values ranging from PPI10 (referred to as "low density") to PPI30 ("high density") were selected to replicate the aerodynamic properties of typical ivy. In addition, the PPI60 ("extreme density") represents an extreme case with significantly reduced permeability and high aerodynamic resistance, intended to mimic artificial greening systems. Furthermore, two vegetation layer thicknesses were considered:  $t = 5$  mm ("thin") and  $t = 10$  mm ("thick").

To quantify the impact of vegetation, Laser Doppler Velocimetry (LDV) was used to analyze flow dynamics. Figure 1 illustrates the model building and the LDV measurement positions. The LDV time record length was  $T = 120$  s, with a sampling rate of  $f = 250$  Hz for measurements in the opening and  $f = 500$  Hz for all other measurements. A comprehensive description of the model and experimental approach, including the description of the vegetation modelling and its scaling, can be found in Pappa et al. (2023b), Pappa et al. (2023a) and Pappa et al. (2025).

### 3 Wind-driven ventilation

Wind-driven ventilation consists of two components: a mean component, driven by the mean pressure field at the ventilation openings (multiple openings with different wind-induced pressures), and a fluctuating component, driven by fluctuating pressures and unsteady flows around the openings (all openings located in regions of similar mean pressure). According

to Straw et al. (2000), the fluctuating component of ventilation can be further divided into distinct ventilation mechanisms. For the configuration investigated here, two components are dominant:

1. **Unsteady continuous airflow** – representing fluctuations in the ventilation flow caused by surface pressure fluctuations at the inflow and outflow openings across a wide frequency range, commonly referred to as broadband ventilation fluctuations.
2. **Eddy penetration** – resulting from fluid transfer due to eddies (turbulence) in unstable shear layers that form when the external flow moves across each opening.

Broadband ventilation fluctuations follow variations in the oncoming wind across a wide range of frequencies. The energy in these fluctuations relates to changes in upstream flow conditions, which may be affected by upstream vegetation. The ventilation rate due to broadband ventilation,  $Q_B$ , can be computed as

$$Q_B = \frac{1}{T} \int_{t=0}^T |Q(t)| dt, \quad (1)$$

where  $T$  is the time series length, and  $Q(t)$  represents the ventilation flow rate time series. While the absolute value in the integral  $|Q(t)|$  ensures that both inflow and outflow contribute positively to the estimated ventilation rate, this formulation assumes unidirectional flow across the opening. However, during eddy penetration events, simultaneous inward and outward flows can occur within different regions of the opening, leading to a net zero flow over the opening area (i.e.,  $Q(t) = 0$ ), and is therefore not accounted for in the velocity-based ventilation metric, despite ongoing fluid exchange, which adds to the total ventilation; see Straw et al. (2000).

For this reason, this study proposes a new metric for quantifying ventilation efficiency, the so-called "penetration metric",  $s_p$ , instead of the typically used ventilation flow rate. The concept behind the penetration metric is to estimate the characteristic size of coherent turbulent structures, such as eddies caused by surface pressure fluctuations or shear layer instability, traversing the opening. It is determined by analyzing the time interval and wall-normal velocity component  $V$  of a continuous series of velocity measurement time steps with inward-directed flow at a specific position in the opening, as indicated by the grey-shaded areas in Figure 2. The assumption is that these continuous events correspond to coherent structures or air jets. However, it should be noted that these structures are not necessarily preserved in their coherent form after traversing the opening. They likely undergo significant deformation or breakdown during the transition, due to interactions with shear layers, pressure gradients, and surrounding turbulence.

Table 1: Foam parameters including thickness, pressure loss coefficient, and corresponding full-scale leaf area density (LAD).

Case	Foam type	Thickness [mm]	Pressure loss coefficient [ $m^{-1}$ ]	LAD [ $m^2/m^3$ ]
low density / thin	PPI10	5	194	2,20
low density / thick	PPI10	10	250	2,80
medium density / thin	PPI20	5	468	5,20
high density / thick	PPI30	10	1000	11,10
extreme density / thick	PPI60	10	2346	26,10

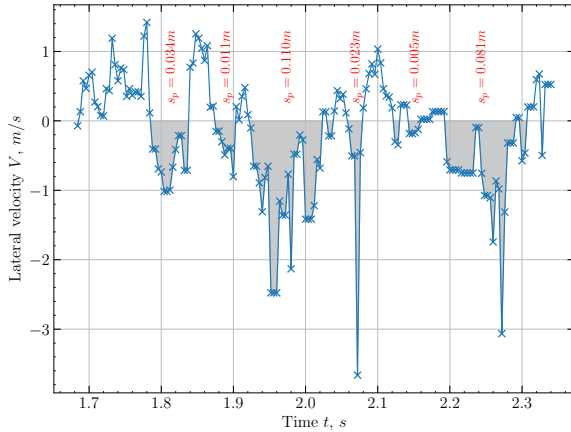


Figure 2: Computation of the “penetration metric”.

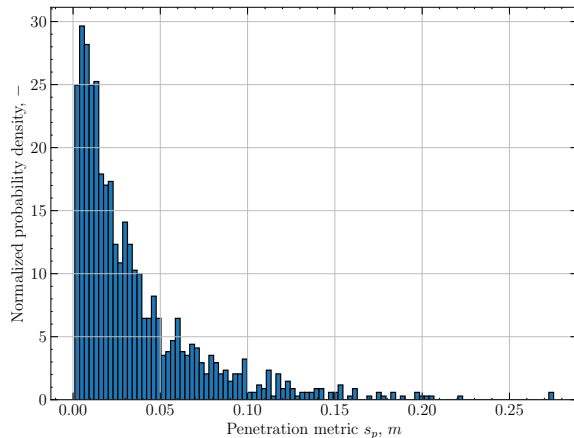


Figure 3: Probability density distribution of the “penetration metric”.

The penetration metric”  $s_p$  is determined by integrating these individual intervals with inward-directed flow, as

$$s_p = \int_{t_1}^{t_2} |v(t)| dt, \quad (2)$$

where  $t_1$  is the start time of the interval,  $t_2$  is the end time, and  $v(t)$  represents the velocity time signal. This way, a length scale is obtained, representing the penetration depth into the opening.

Figure 3 visualises the probability density distribution of the penetration depth at the central position of the opening for the bare case, i.e., without any vegetation on the building façade. The distribution is strongly right-skewed, indicating a large number of short penetration events and a long tail ex-

tending towards higher values. This pattern reflects the intermittent nature of turbulent ventilation, where most coherent structures penetrate only slightly into the opening, while some rare but significant events were observed with a very long duration, as caused by large-scale structures or very intense gusts with a high velocity. The most frequent value is approximately  $s_p = 0.01$  m, suggesting that the majority of coherent structures transfer air only about 1 cm across the opening into the interior.

## 4 Results

In the following, the effect of vegetation on the flow around the model and within the opening is first analysed in detail, followed by the application of the “penetration metric” to estimate the influence of vegetation on the ventilation of the interior space.

### Effect of vegetation on external and internal flow

Figures 4–6 show the time-averaged lateral velocity component at various distances from the side wall for all investigated positions (SA to SC; see Figure 1). For the reference case “bare” (without vegetation) and the “high density / thick” case, violin plots are included, illustrating the probability density of velocity data at different magnitudes. The broad velocity spread in the probability density highlights the transient nature of the flow around the model, which is visible in all investigated cases. While the mean time-averaged velocity (denoted by a cross in the plots) is generally consistent among the cases, except for the “extreme density / thick” case, the vegetation notably influences the distribution shape, resulting in a narrower distribution close to the wall.

Comparing the velocity distribution for the different investigated streamwise positions (SA, SB, and SC in Figures 4-6) and various vegetation types reveals that the effect of vegetation is most pronounced near the upstream corner of the model (position SA). At the downstream positions (SB and SC), the lateral velocity component exhibits similar levels across all investigated cases, indicating a diminished impact of the façade vegetation further downstream.

Additionally, the flow time series for the measurement position closest to the side wall (distance from the wall 5 mm) was analyzed using the power spectral density of the lateral velocity, shown in Figures 7-9 for all three investigated positions along the side wall. The effect of vegetation extends across the entire fre-

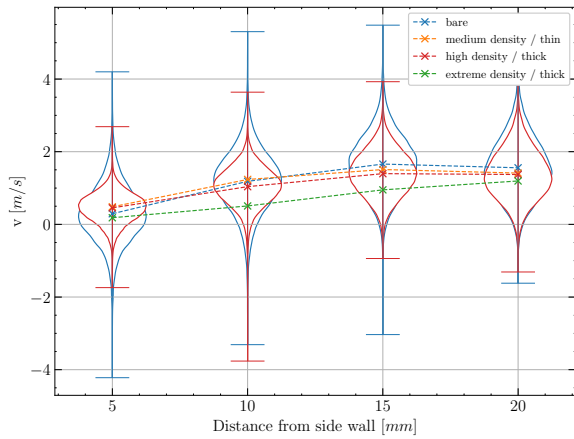


Figure 4: Experimental results for the lateral flow velocity at position SA

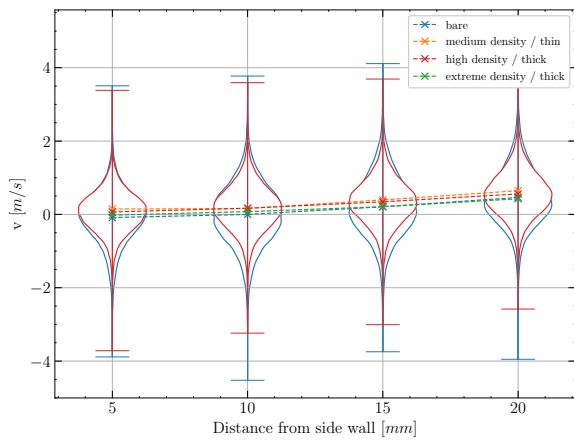


Figure 5: Experimental results for the lateral flow velocity at position SB

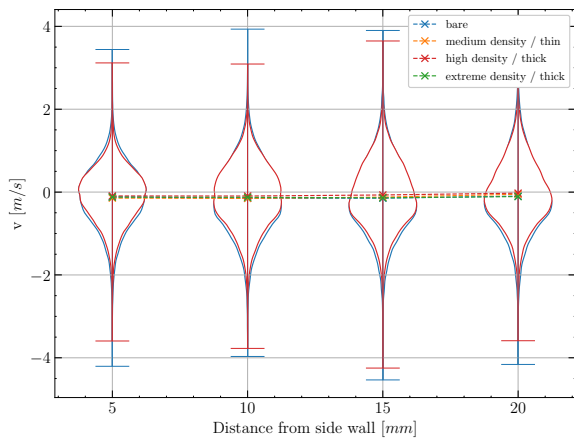


Figure 6: Experimental results for the lateral flow velocity at position SC

quency range for the position SA closest to the upwind corner of the model, with the greatest impact observed at frequencies above  $f = 3$  Hz, reaching into the inertial subrange. This highlights the role of vegetation in modifying turbulent eddies that develop at the upstream corner of the cube model. The reduction of high-frequency fluctuations indicates that vegetation primarily dampens small-scale turbulent structures, reducing overall turbulence intensity near the

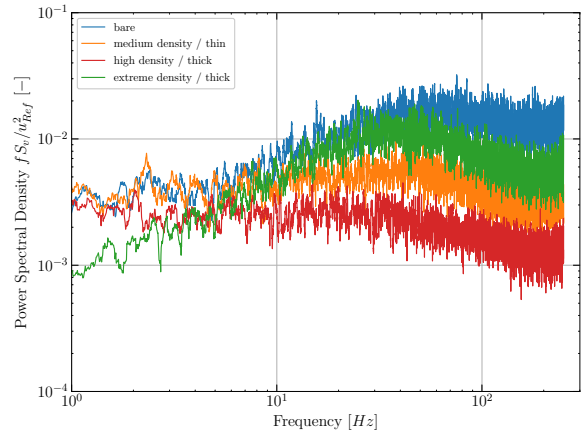


Figure 7: Power spectral density of the measurement point located 5 mm from the wall for position SA

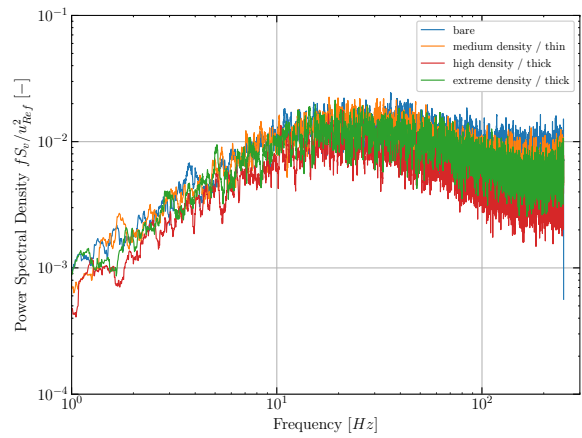


Figure 8: Power spectral density of the measurement point located 5 mm from the wall for position SB

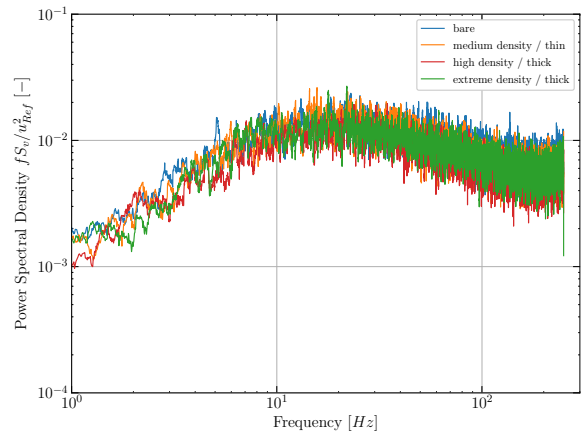


Figure 9: Power spectral density of the measurement point located 5 mm from the wall for position SC

side wall. Additionally, the differences between vegetation cases suggest that denser and thicker vegetation configurations are more effective in decreasing fluctuations, especially at higher frequencies, which is consistent with the increased aerodynamic resistance introduced by those vegetation elements. However, the "extreme density / thick" case represents a very dense vegetation coverage, almost to a degree that it acts as a nonporous material, where turbulent eddies are unable

to penetrate as effectively as in the less dense "low" to "high" cases. The same effect has been observed in pressure measurements in Pappa et al. (2025). As a result, the damping effect on turbulent eddies is less pronounced. Furthermore, for the "extreme density / thick" case, the power spectral density in the very low-frequency range deviates from the other investigated cases. This discrepancy arises because the addition of an almost impermeable vegetation layer to the upstream façade effectively elongates the model in the streamwise direction, thereby basically shifting the position SA downstream by the thickness of the vegetation layer. As a result, the spectral characteristics observed at position SA for this case closely resemble those found at position SB.

The results for the roof (not shown here) exhibit the same general trends as those observed along the side wall, with the most pronounced influence of vegetation occurring near the upstream corner of the model. A comparison of the flow characteristics at position RB on the roof and position SB along the side wall, both located at the same downstream position, shows that vegetation has a more pronounced effect on the roof flow than on the side wall. This is likely due to the proximity of the side wall flow to the ground, which introduces additional damping effects and restricts the development of turbulence.

For the flow configuration investigated here, where the openings are oriented parallel to the main flow direction, the time-averaged mean velocity within the opening, based on LDV results, is effectively zero. This is illustrated in Figure 10, which presents the time-averaged lateral velocity component at three central positions within the opening, located at heights of  $h = 50, 60,$  and  $70$  mm above the floor. Additionally, for the "bare" and the "high density / thick" vegetation case, violin plots are included in Figure 10. The broad velocity distribution observed in the probability density within the opening confirms that fluctuating ventilation is the dominant transport mechanism. Furthermore, the power spectral density of the lateral velocity component at the centre of the opening – measured at a height of  $60$  mm – is presented in Figure 11. The spectral characteristics closely resemble those of the external sidewall flow, indicating again that vegetation primarily dampens small-scale turbulent structures. These high-frequency fluctuations originate in the outdoor flow field and are transmitted through the opening into the building interior.

The results for the wake (not shown here) confirm that vegetation influences only the upstream flow, as neither the time-averaged vertical velocity component nor the corresponding probability distributions (violin plots) exhibit any significant differences between the investigated cases.

#### Application of the "penetration metric"

The ventilation rate ratio,  $Q_{B,Veg.}/Q_{B,Bare}$ , can be compared to the total ventilation rate ratio obtained

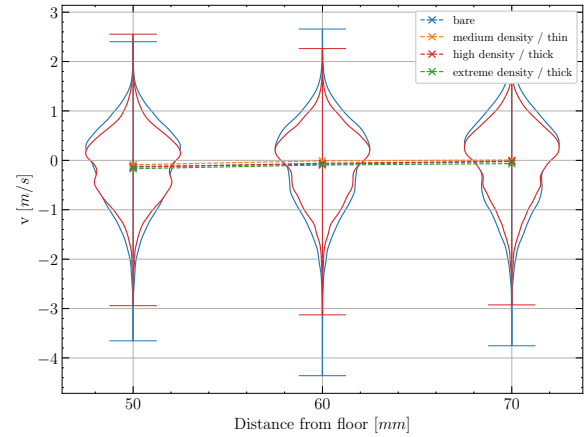


Figure 10: Experimental results for the lateral flow velocity in the opening for three different heights.

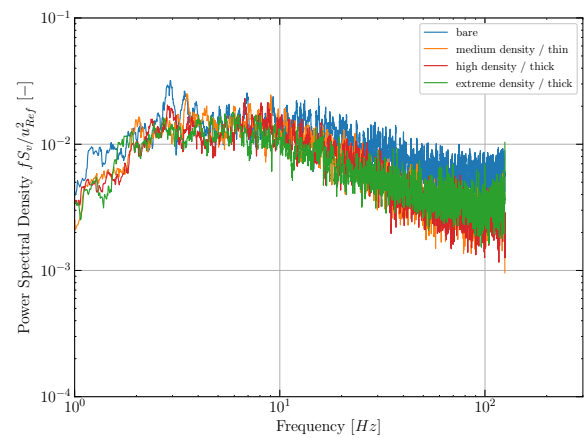


Figure 11: Power spectral density of the measurement point at the central position in the opening.

from tracer gas measurements ( $I$  being the total ventilation rate), as presented in Pappa et al. (2023b) for the same geometry and vegetation cases, along with the penetration metric ratio,  $s_{P,Veg.}/s_{P,Bare}$ , proposed in this study. The penetration metric was evaluated for all investigated positions in the opening, according to equation 2, and then averaged. Figure 12 presents a comparison of these ratios for all investigated vegetation cases. The broadband ventilation flow rate ( $Q_B$ ) alone does not fully account for the total ventilation rate. The discrepancy with the corresponding tracer gas measurements ( $I$ ) arises because  $Q_B$  does not capture the contribution of eddy penetration, aligning closely with the findings of Straw et al. (2000).

However, the proposed metric  $s_P$  reasonably accounts for the contributions from both broadband ventilation and eddy penetration, as evidenced by its excellent agreement with the tracer gas measurements shown in Figure 12. This agrees with the prominent effect of the eddy penetration mechanism in this particular case via the previously discussed notable effect of vegetation on small scale turbulent structures observed near the upstream corner.

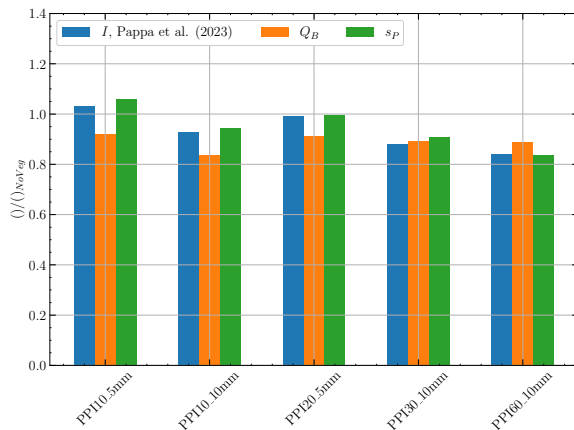


Figure 12: Effect of façade vegetation on the ventilation metrics.

## 5 Conclusions

The flow around a model building with various vegetation types mounted on its upstream façade was experimentally investigated in an atmospheric boundary layer wind tunnel representing urban flow conditions.

Analysis of the mean flow characteristics and power spectral density indicated that the primary effect of vegetation is limited to the upstream region of the model, as evidenced by dampened small-scale turbulent structures. However, its influence on turbulent eddies remains noticeable further downstream.

The present study introduces the "penetration metric" and demonstrates its ability to capture the effect of vegetation on small-scale turbulent structures in the flow.

A comparison of different ventilation efficiency metrics demonstrated that the penetration metric effectively accounts for all relevant ventilation mechanisms. It shows excellent agreement with tracer gas measurements and therefore serves as a more comprehensive measure of ventilation efficiency.

## Acknowledgements

This work was co-funded by the European Union under the Horizon Research and Innovation Programme WIDERA 2021-ACCESS-03-01 (Project "TWEET-IE", GA#: 101079125).

## References

Albuquerque, D. P., M. Sandberg, P. Linden, and G. Carilho da Graça (2020). "Experimental and numerical investigation of pumping ventilation on the leeward side of a cubic building". In: *Building and Environment* 179, p. 106897.

Balczó, M., C. Gromke, and B. Ruck (2009). "Numerical modeling of flow and pollutant dispersion in street canyons with tree planting". In: *Meteorologische Zeitschrift* 18.2, p. 197.

Bu, Z., S. Kato, and T. Takahashi (2010). "Wind tunnel experiments on wind-induced natural ventilation rate in residential basements with areaway space". In: *Building and Environment* 45.10, pp. 2263–2272.

Karava, P., T. Stathopoulos, and A. Athienitis (2011). "Air-flow assessment in cross-ventilated buildings with operable façade elements". In: *Building and Environment* 46.1, pp. 266–279.

Larsen, T. S. and P. Heiselberg (2008). "Single-sided natural ventilation driven by wind pressure and temperature difference". In: *Energy and Buildings* 40.6, pp. 1031–1040.

Li, H., Y. Zhao, B. Sützl, A. Kubilay, and J. Carmeliet (2022). "Impact of green walls on ventilation and heat removal from street canyons: Coupling of thermal and aerodynamic resistance". In: *Building and Environment* 214, p. 108945.

Manolesos, M., Z. Gao, and D. Bouris (2018). "Experimental investigation of the atmospheric boundary layer flow past a building model with openings". In: *Building and Environment* 141, pp. 166–181.

Pappa, V., C. Gromke, and D. Bouris (2023a). *Twin test I: Effect of vegetation on urban flows. PIV data from NTUA WT experiment and LDV from KIT WT experiment*. Version 1.0.0. Data set.

Pappa, V., A. Bakolas, D. Bouris, and C. Gromke (2025). "Effects of Façade and Rooftop Greening on the Surface Pressure Distribution of an isolated Cubic Building with Side Wall Apertures." In: *Accepted for publication in Journal of Wind Engineering and Industrial Aerodynamics*.

Pappa, V., D. Bouris, W. Theurer, and C. Gromke (2023b). "A wind tunnel study of aerodynamic effects of façade and roof greening on air exchange from a cubic building". In: *Building and Environment* 231, p. 110023.

Stenech, M., G. Decitre, G. Brenn, and C. Irrenfried (2025). "Experimental investigation of the ventilation efficiency for single-sided ventilation in suburban areas". In: *Building and Environment* 283, p. 113280.

Straw, M., C. Baker, and A. Robertson (2000). "Experimental measurements and computations of the wind-induced ventilation of a cubic structure". In: *Journal of Wind Engineering and Industrial Aerodynamics* 88.2-3, pp. 213–230.